Supplemental Document

Biomedical Optics EXPRESS

Four-color fluorescence cross-correlation spectroscopy with one laser and one camera: supplement

SONALI A. GANDHI,[1] MATTHEW A. SANDERS,[2] JAMES G. GRANNEMAN,[2,3] AND CHRISTOPHER V. KELLY[1,3,*]

[1] *Department of Physics and Astronomy, Wayne State University, Detroit, MI 48201, USA*
[2] *Center for Molecular Medicine and Genetics, School of Medicine, Wayne State University, Detroit, MI 40201, USA*
[3] *Center for Integrative Metabolic and Endocrine Research, School of Medicine, Wayne State University, Detroit, MI 48201, USA*
[*] *cvkelly@wayne.edu*

Supplement DOI: https://doi.org/10.6084/m9.figshare.22632871

Parent Article DOI: https://doi.org/10.1364/BOE.486937

Four-color fluorescence cross-correlation spectroscopy with one laser and one camera

SONALI A. GANDHI[1], MATTHEW A. SANDERS[2], JAMES G. GRANNEMAN[2,3], AND CHRISTOPHER V. KELLY[1,3,*]

[1]*Department of Physics and Astronomy, Wayne State University, Detroit, MI, USA, 48201*
[2]*Center for Molecular Medicine and Genetics, School of Medicine, Wayne State University, Detroit, MI, USA, 40201*
[3]*Center for Integrative Metabolic and Endocrine Research, School of Medicine, Wayne State University, Detroit, MI, USA. 48201*
*cvkelly@wayne.edu

Supplemental Methods

Protein purification

Baculovirus for protein expression were prepared using the Bac-to-Bac expression system (Invitrogen). pFastBac1 constructs for PLIN5-YFP-His tag (all mouse protein) was made using standard molecular biological methods and was confirmed by sequencing. Bacmid DNAs were generated by transformation of DH10Bac E. coli (Invitrogen) with FastBac plasmids following the manufacturer's protocol. Initial baculovirus stocks were generated by transfection of Sf9 insect cells with bacmid DNA using Cellfectin II reagent (Invitrogen) according to the manufacturer's protocol, then were amplified by infection of Sf9 cells with the initial baculoviral stocks.

Amplified baculoviral stocks were used to infect High Five insect cells and cells were collected 48 hrs after start of infection when cells were ~80% viable. High Five cells expressing proteins were lysed by sonication in IB containing 20 ug/mL leupeptin and pepstatin A. For PLIN5-YFP-His tag preparations, 0.5% FOS-CHOLINE-12 detergent (Anatrace) was added to sonicated cell extracts prior to centrifugation at 10,000 g. Supernatants were then incubated with TALON Cobalt beads (Takara) for two hours at room temperature, then proteins were eluted from beads using 50 mM sodium phosphate buffer pH 7.4 containing 150 mM imidazole. Imidazole was removed from proteins by successive rounds of concentration and redilution with IB using Centricon centrifugal filter units of the appropriate molecular weight cutoff. Protein concentration was determined by BCA (Pierce), then protein purity was determined from Coomassie-stained PAGE gels.

Triple cross-correlation data analysis

For the multi-color aggregation with more than two spectrally resolved molecules, three or four intensity versus time signals may be considered in a single cross-correlation analysis with two or three independent lag times, respectively,(39–42) according to

$$G_{C3}(\tau_1,\tau_2) = \frac{\langle \delta I_1(t)\, \delta I_2(t+\tau_1)\, \delta I_3(t+\tau_2)\rangle}{\langle I_1(t)\rangle \langle I_2(t)\rangle \langle I_3(t)\rangle} \quad \text{(S1)}$$

$$G_{C4}(\tau_1,\tau_2,\tau_3) = \frac{\langle \delta I_1(t)\, \delta I_2(t+\tau_1)\, \delta I_3(t+\tau_2)\, \delta I_4(t+\tau_3)\rangle}{\langle I_1(t)\rangle \langle I_2(t)\rangle \langle I_3(t)\rangle \langle I_4(t)\rangle} \quad \text{(S2)}$$

With a complex, non-uniform aggregation process, these high-order cross-correlations may provide insightful details into which colors are mixing into or out of the aggregates. The data collected for this manuscript did not yield specific insights from Eq. S1 or S2 because the nanobeads and LUVs seemingly all acted similarly to each other; they all diffused independently until PBS or BSA were added, after which they all participated in the aggregation. However, these higher-order cross-correlations may prove to be useful when more than two intensities versus time are available.

FCS detection volume characterization and approximation

The ellipsoid of FCS detection volume may be characterized according to exponential decay in detection probability in both the radial (r) and optical (z) axes according to

$$W(r,z) = \frac{2}{r_0\, z_0\, \pi}\exp\left(-2\frac{r^2}{r_0^2}\right)\exp\left(-2\frac{z^2}{z_0^2}\right) \quad \text{(S3)}$$

dependent on the radial (r_0) and optical-axis (z_0) extent of detection. The detection probability was approximated by the square of a Gaussian beam intensity, which given by

$$I(r,z) = \mathrm{I}_0\left(\frac{w_0}{w(z)}\right)^2\exp\left(-2\frac{r^2}{w(z)^2}\right) \quad \text{(S4)}$$

Dependent on the beam waist (w_0) and the z-dependent beam waist ($w(z)$) given by

$$w(z) = w_0\left(1+\left(\frac{z}{z_R}\right)^2\right)^{\frac{1}{2}} \quad \text{(S5)}$$

The Rayleigh length (z_R) that is given by

$$z_R = n\frac{w_0}{NA}. \quad \text{(S6)}$$

In our setup, the numerical aperture (NA) was 1.3 and the index of refraction of the immersion oil (n) was 1.518. The $I(r,z)^2$ approximates $W(r,z)$ when $r_0 = w_0$ and $z_0 = z_R / \sqrt{2}$. The beam waists for each color excitation laser were measured by imaging uniformly labeled supported lipid bilayers illuminated by the excitation lasers (Fig. S1).

Supplemental Figures

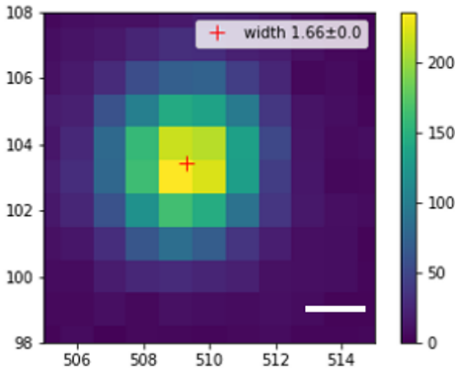

Figure S1: Laser spot size for λ_{ex} = 561 nm. Scalebar = 0.12 µm.

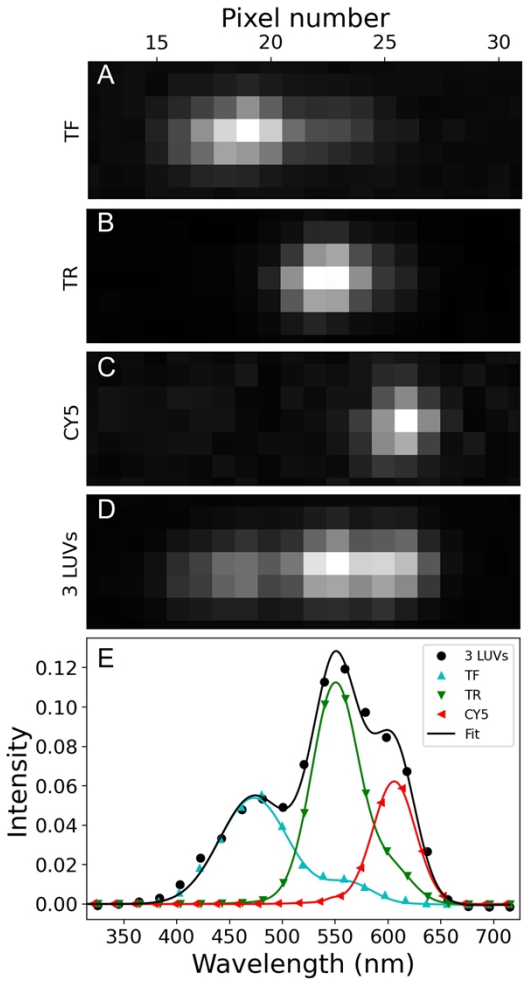

Figure S2: The emission spectra of the LUVs on the camera sensor. (A-C) Single LUVs TF, TR and CY5 of excitation wavelengths 515, 561 and 635 nm, respectively, were spectrally separated and collected on the cropped ROI (18x6). Each column of pixels on the camera is associated with an emission wavelength. (D) Samples with all three LUVs show the distinct, but highly overlapping emission spectra. (E) Control samples with only one color of LUV present were used to identify the emission spectrum of each LUV type (colored symbols and fits). With three LUVs simultaneously present, the spectrum was fit to reveal the emission intensity of each LUV type for each camera frame (black symbols and fit).

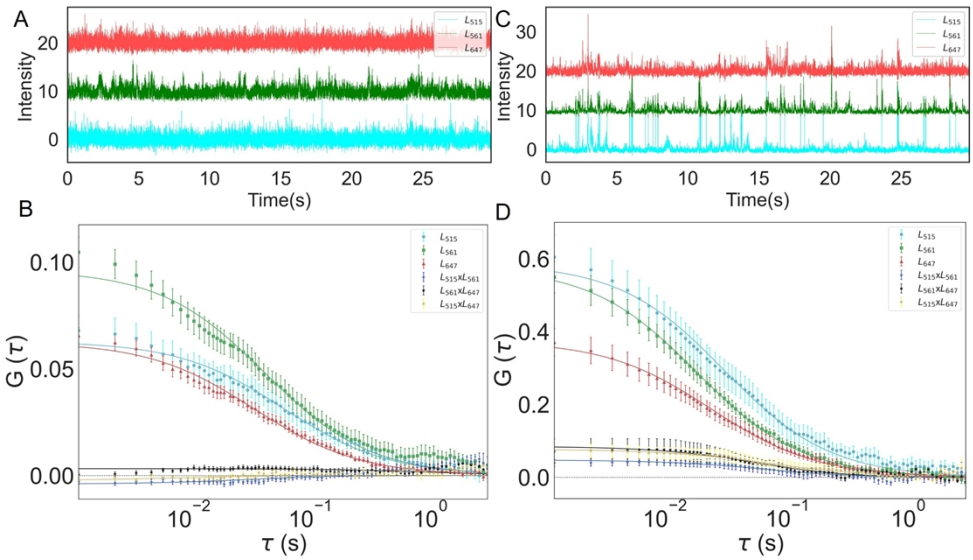

Figure S3: LUVs form homo-and hetero-aggregates with addition of BSA. (A) Intensity versus time for three LUVs (TF, TR, CY5) in water shows many small uncorrelated peaks that confirm LUVs are diffusing independently. (B) G versus τ reports auto correlations were significant whereas cross-correlations were unclear. (C) Addition of BSA induces aggregation of LUVs, intensity versus time for three color channel shows many events of correlated peaks. (B) G versus τ reports both auto and cross-correlations were significant, induced aggregation cause increase in auto- and cross-correlations. Symbols and error bars represent the mean and standard error of the mean for >7 sequential measurements while the lines represent the fits from Eq. 7.

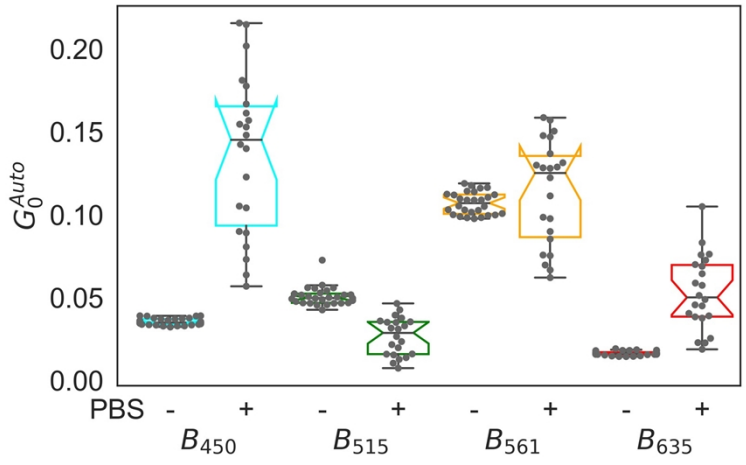

Figure S4: Addition of PBS induced nanobead aggregates. PBS addition resulted in a reduction of the number of diffusers for most color channels.

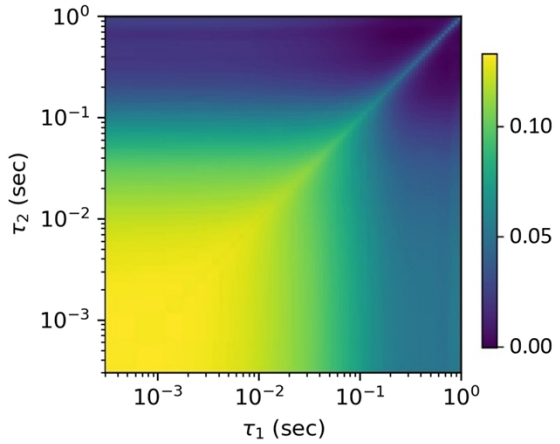

Figure S5: Contour plots of three-color cross-correlation decay for the B515, B561, and B635 nanobeads in PBS. The symmetry of this plot demonstrates the consistent aggregation between the beads with no bead being excluded from the aggregates or being correlated with different aggregate diffusion characteristics.

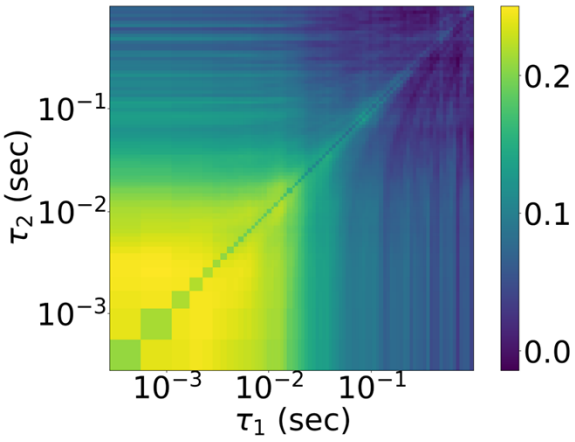

Figure S6: Contour plot of three-color cross-correlation decay for LUVs (TF, TR, CY5).

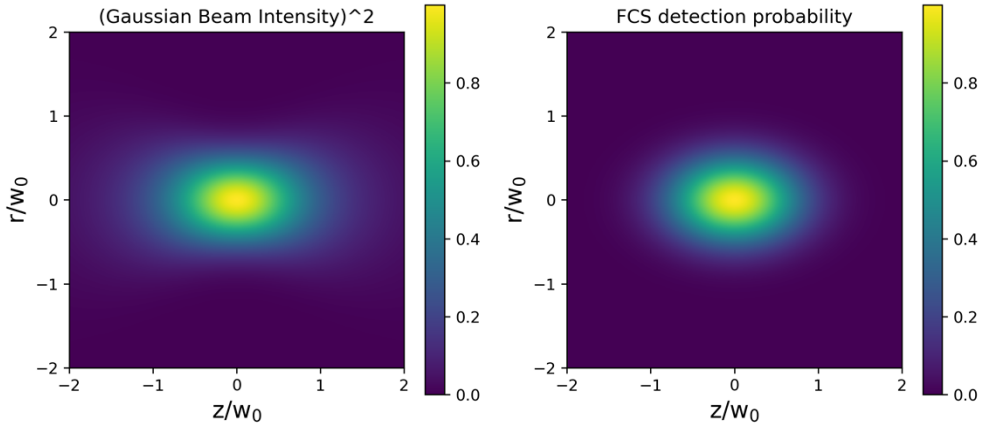

Figure S7: A demonstrated similarity between the square of the Gaussian beam intensity (Eq. S4) and the normalized FCS detection volume (Eq. S3) for the optical parameters used in our setup.

Supplemental Tables

Table S1: Details of the nanobeads used in these experiments.

Beads	Size (nm)	Color	Coating	Surface charge	Manufacturer	Lot number
B_{450}	100	Blue	Polystyrene	Neutral	Thermo Fisher	184539
B_{515}	100	Yellow	Carboxylate	Negative	Life Technologies	1588588
B_{515}	40	Yellow	Carboxylate	Negative	Life Technologies	1600256
B_{561}	100	Red	Polystyrene	Neutral	Thermo Fisher	180315
B_{561}	200	Red	Polystyrene	Neutral	Thermo Fisher	40704
B_{635}	40	Dark red	Carboxylate	Negative	Life Technologies	1437595

Table S2: Comparison of LUV diffusion, diameter, and aggregate fraction.

LUV Type	Diameter after extrusion (nm)	D_{Theory} (μm^2/sec)	D_{Exp} (μm^2/sec)		Estimated diameter (nm)		Aggregate fraction (%)
			Water	BSA	Water	BSA	BSA
TF	100	4.39	0.63 ± 0.04	1.06 ± 0.07	740 ± 90	440 ± 50	99.9
TR	100	4.39	1.03 ± 0.06	1.76 ± 0.08	450 ± 50	260 ± 20	91.8
Cy5	100	4.39	1.01 ± 0.02	1.10 ± 0.12	426 ± 18	360 ± 70	77.2